Supplement of Atmos. Chem. Phys., 26, 15813–15830, 2026
https://doi.org/10.5194/acp-26-15813-2026-supplement
© Author(s) 2026. CC BY 4.0 License.



Atmospheric Chemistry and Physics
Open Access
EGU

Supplement of

Revisiting the parameterization of ice nucleation of dust particles under mixed-phase cloud conditions from laboratory measurements

Jie Chen and Zamin A. Kanji

Correspondence to: Jie Chen (jie.chen@env.ethz.ch) and Zamin A. Kanji (zamin.kanji@env.ethz.ch)

The copyright of individual parts of the supplement might differ from the article licence.

Table S1. Ice nucleation parameterizations of immersion mode dust particles compiled from previous studies, including both Classic Nucleation Theory (CNT)-based and empirical parameterizations.

Reference	Particle Type	Parameterizations
CNT-based parameterizations (J_{het} in the unit of s^{-1})		
Marcolli et al. (2007) Chen et al. (2008) Murray et al. (2011) Niedermeier et al. (2011a) Savre and Ekman (2015)	Arizona Test Dust (ATD) Hematite/corundum Illite, natural dust	$J_{het}(T) = A \times exp(\frac{-\Delta G_{act} - \Delta G_g f(\theta)}{kT})$ $f(\theta) = \frac{(2+cos\theta)(1-cos\theta)^2}{4}$ J_{het}: heterogenous ice nucleation rate (i.e., the number of nucleation events per unit particle surface and unit time) A: a pre-exponential factor k: the Boltzmann constant ΔG_{act}: the activation energy required for water molecule reoritention ΔG_g: the Gibbs free energy required to form a critical ice embryo $f(\theta)$: the shape factor determined by the contact angle (θ) between the critical ice embryo and INP surface. θ is given based on the surface properties of particles and thus varies across studies. For example, Chen et al. (2008) assumed a specific θ value for each aerosol component, whereas several other studies(Savre and Ekman, 2015; Niedermeier et al., 2011a) represented θ for each component using a probability density function
Empirical parameterizations (n_s in the unit of m^{-2})		
Niemand et al. (2012)	Desert dust	$n_s(T) = \exp(8.934 - 0.517T)$, $T \in$ [-36, -12] ℃
Atkinson et al. (2013)	K-feldspar	$n_s(T) = 10000 \times \exp(275.26 - 1.038T)$, $T \in$ [248, 268] K
Kanji et al. (2013b)	Unaged and O_3 aged Kaolinite (Ka) and ATD	Unaged Ka: $n_s(T) = \exp(116.3 - 0.38T)$, $T \in$ [233, 264] K Unaged ATD: $n_s(T) = \exp(79.4 - 0.21T)$, $T \in$ [233, 264] K
Augustin-Bauditz et al. (2014)	Feldspar and illite	Feldspar: $n_s(T) = 0.0155 \times \exp(-0.824T)$, $T \in$ [-29, -23] ℃ illite: $n_s(T) = 37.066 \times \exp(-0.353T)$, $T \in$ [-37, -28] ℃
DeMott et al. (2015)	Natural dust from both laboratory and field measurements	$N_{\mathrm{INP}}(T) = cf(n_{>0.5\,um})^{(\alpha(273.16-T)+\beta)}\exp(\gamma(273.16-T)+\delta)$, N_{INP} is the number concentration of INPs in air (std L^{-1}), $T \in$ [238, 253] K cf =1, α=0, β=1.25, γ=0.46, δ=-11.6
Broadley et al. (2012)	illite rich particles	$n_s(T) = \exp(6.53043 \times 10^4 - 8.2153088 \times 10^2 T + 3.446885376T^2 - 4.822268 \times 10^{-3}T^3)$, $T \in$ [236.2, 247.5] K
Ullrich et al. (2017)	Ground desert dust	$n_s(T) = \exp(150.577 - 0.517T)$, $T \in$ [243, 259] K

Harrison et al. (2019)	Quartz	$n_s(T) = \exp(-1.709 + 7 \times 10^{-2}T + 1.75 \times 10^{-2}T^2 + 2.66 \times 10^{-4}T^3)$, $T \in$ [-37.5, -10.5] ℃

Table S2. Summary of studies included in the ice nucleation dataset utilized for this work.

References	Methods	Residence time or cooling rate	Particle/Droplet size (diameter/ volume)	Dust species	Aging treatments
Salam et al. (2007)	Aerosol	20 s	1 μm	Montmorillonite	NH_3 gas exposure (25 ppm, 100%)
Sullivan et al. (2010a)	Aerosol	5 s	200 nm	ATD A1	HNO_3 gas exposure
Sullivan et al. (2010b)	Aerosol	5 s	300 nm	ATD A1	H_2SO_4 coating at 70 ℃ Heating at 250 ℃
Murray et al. (2011)	Suspension	0.8–10	10–50 μm	Kaolinite	Unaged
Niedermeier et al. (2011b)	Aerosol	1.6 s	300 nm	ATD A1	H_2SO_4 coating at 45, 70, 80 ℃, $(NH_4)_2SO_4$ coating Heating at 250 ℃
Tobo et al. (2012)	Aerosol	5 s	300 nm	Kaolinite	Levoglucosan coating, H_2SO_4 coating
Kanji et al. (2013a)	Aerosol	10 s		ATD nomial (0-3 μm), Kaolinite (KGa-1b)	O_3 gas exposure
Atkinson et al. (2013)	Suspension	1 ℃ min^{-1}	14–16 μm and 1 μL	Feldspar, Quartz, Montmorillonite, Chlorite	Unaged
Wex et al. (2014)	Aerosol	1.6 s	300 or 700 nm	Kaolinite (Fluka, CMS)	Levoglucosan coating
Augustin-Bauditz et al. (2014)	Aerosol	1.6 s	300 nm	ATD A1, K-feldspar, illite, Kaolinite	H_2SO_4 coating at 70 ℃
Sihvonen et al. (2014)	Aerosol	-	2.5 μm	Kaolinite (KGa-1b)	H_2SO_4 aqueous reaction, HNO_3 aqueous reaction
Kulkarni et al. (2014)	Aerosol	12 s	200 nm	ATD A1, illite, K-feldspar, Montmorillonite	H_2SO_4 coating
Kulkarni et al. (2015)	Aerosol	12 s	200 nm	ATD A1, illite, K-feldspar	HNO_3 coating
Emersic et al. (2015)	Aerosol	-		illite, K-feldspar, Kaolinite	Unaged
Hiranuma et al. (2015)	Aerosol and Suspension	-	Different instruments	illite NX	Unaged
Zolles et al. (2015)	Suspension	0.1−10 ℃ min^{-1}	10−40 μm	Kaolinite, Quartz, Montmorillonite, ATD (not indicated), Volcanic ash	Unaged

Peckhaus et al. (2016)	Suspension	1 °C min^{-1}	215±70 pL	Na-feldspar, K-feldspar	Water aging, H_2O_2 solution, Heating at 90 °C
Harrison et al. (2016)	Suspension	1 °C min^{-1}	1 µL	different feldspars	Unaged, water aging with different time
Boose et al. (2016)	Aerosol	10 s	< 2.5 µm	9 desert dust	Unaged
DeMott et al. (2018)	Aerosol	Different instruments	Polydisperse	illite NX, Sahara desert dust, K-feldspar	Unaged
Perkins et al. (2019)	Suspension	0.3 °C min^{-1}	50 µL	ATD A2	Water, salt solutions (NaCl, KCl, Sea salt), acid solutions (HCl, H_2SO_4, HNO_3), peroxide, Heating at 500 and 600 °C
Harrison et al. (2019)	Suspension	1 °C min^{-1}	1 µL	Different types of quartz	Water aging, air aging
Kanji et al. (2019)	Aerosol	5 s	Polydisperse	Natural desert dust	α-Pinene secondary organic aerosol coating
Fahy et al. (2022)	Suspension	1 °C min^{-1}	1 µL	Volcanic ash	Water, H_2SO_4 solution
Chen et al. (2023)	Suspension	1 °C min^{-1}	1 µL	ATD nomial (0-3 µm), K-feldspar	NO_2 gas exposure

Table S3. Summary of ice nucleation metrics derived for each study, indicating whether values were calculated in this work, extracted directly from literature, or not available.

References	Ice active site surface density (n_s)	Source (derived or reported from literature)	Ice nucleation rates (J_{het})	Source (derived or reported from literature)
Salam et al. (2007)	Yes	Calculated	Yes	Calculated
Sullivan et al. (2010a)	Yes	Calculated	Yes	Calculated
Sullivan et al. (2010b)	Yes	Calculated	Yes	Calculated
Murray et al. (2011)	Yes	From the literature	Yes	From the literature
Niedermeier et al. (2011b)	Yes	Calculated	Yes	Calculated
Tobo et al. (2012)	Yes	Calculated	Yes	Calculated
Kanji et al. (2013a)	Yes	From the literature	Yes	Calculated
Atkinson et al. (2013)	Yes	From the literature	No	
Wex et al. (2014)	Yes	From the literature	Yes	From the literature
Augustin-Bauditz et al. (2014)	Yes	Calculated	Yes	Calculated
Sihvonen et al. (2014)	No	-	No	-
Kulkarni et al. (2014)	Yes	Calculated	Yes	Calculated
Kulkarni et al. (2015)	Yes	Calculated	Yes	Calculated
Emersic et al. (2015)	Yes	From the literature	No	
Hiranuma et al. (2015)	Yes	From the literature	Yes	From the literature
Zolles et al. (2015)	Yes	From the literature	No	
Peckhaus et al. (2016)	Yes	From the literature	Yes	Calculated
Harrison et al. (2016)	Yes	From the literature	Yes	Calculated
Boose et al. (2016)	Yes	From the literature	Yes	Calculated
DeMott et al. (2018)	Yes	From the literature	No	
Perkins et al. (2019)	Yes	Calculated	No	
Harrison et al. (2019)	Yes	From the literature	Yes	Calculated
Kanji et al. (2019)	Yes	From the literature	Yes	Calculated

Fahy et al. (2022)	Yes	From the literature	Yes	Calculated
Chen et al. (2023)	Yes	From the literature	Yes	Calculated

Table S4. Ice formation parameterizations of dust particles, specific for different dust species (illite, kaolinite, feldspar, natural dust, ATD and quartz), measurement methods (aerosol versus suspensions) and aging process.

		T (°C)	R^2	A	B
$\log(n_s) = A \times T + B$					
All dust	Suspension	-41< T <-18	0.50	-0.33986	-0.85008
	Suspension	-18< T <-2	0.12*	-0.08606	3.65451
	Aerosol	-41<T<-2	0.30	-0.12081	7.18228
Unaged all dust (Fresh)	Suspension	-41< T <-18	0.47	-0.31916	-0.17771
	Suspension	-18< T <-2	0.04*	-0.05415	4.17187
	Aerosol	-41<T<-2	0.38	-0.14402	6.44128
Aged all dust	Suspension	-39< T <-18	0.26	-0.34668	-1.24705
	Suspension	-18< T <-2	0.20	-0.10062	3.43158
	Aerosol	-41<T<-2	0.07*	-0.05271	9.53126
Illite	Suspension	-35< T <-10	0.82	-0.46006	-3.67996
	Aerosol	-40< T <-18	0.60	-0.18826	4.93956
Kaolinite	Suspension	-35< T <-20	0.81	-0.28649	0.77669
	Aerosol	-41 < T <-21	0.59	-0.18533	4.77043
Montmorillonite	Suspension	-38< T <-21	0.92	-0.28748	0.04953
	Aerosol	-35< T <-15	0.31	-0.11235	7.94544
K-Feldspar	Suspension	-30 < T <-2	0.78	-0.28628	2.64802
	Aerosol	-39< T <-17	0.31	-0.10158	8.76581
Other feldspars	Suspension	-32< T <-3	0.27	-0.17224	2.15912
ATD	Suspension	-29< T <-2	0.60	-0.18769	2.61687
	Aerosol	-40< T <-12	0.02*	-0.02173	10.92143
Quartz	Suspension	-40< T <-5	0.68	-0.22565	1.47175
$\log(J_{het}) = A \times T + B$					
All dust	Suspension	-41< T <-18	0.54	-0.43815	-4.96807
	Suspension	-18< T <-2	0.01*	-0.02508	2.27726
	Aerosol	-41<T<-2	0.34	-0.14716	5.32369

"*" For these measurements, **a weak correlation between $\log(n_s)$ and temperature has been observed**, where R^2 are smaller than 0.2. For aerosol measurements, this weak correlation is attributed to the limited and highly variable n_s data obtained from dust particles with different compositions (Figure 2) and from aging processes (Figure 6). For

suspension measurements, it arises from the weak temperature dependence of n_s at $T >$-18 °C (Figure 3). Therefore, **these parameterizations should be applied with caution**, as the poor correlation between n_s and T may introduce substantial biases.

To apply the aerosol n_s parameterizations across the full mixed-phase cloud temperature range, the aerosol fits for bulk aerosol were extrapolated up to −2 °C.

Text S1. We conducted two types of significance analysis, including Analysis of Covariance (ANCOVA) to assess the overall difference in ice nucleation ability (INA) between unaged and aged samples across temperatures and Mann-Whitney U-test to assess this difference within individual temperature bin of 1 °C.

To ensure a robust comparison, ANCOVA was strictly restricted to the shared overlapping temperature ranges where data for both unaged and aged samples exist (-42 < T < -20 °C for aerosol measurements and -28 < T < -2 °C for suspension measurements). The ANCOVA results yielded a highly significant difference (p<0.05) between aerosol measurements and suspension measurements. This indicates that the aging process significantly alters the INA temperature dependence of dust particles.

The results of U-test within individual temperature bins (1 °C) are shown in the tables below for aerosol (Table S5) and suspension measurements (Table S6), respectively. As shown in the tables, a statistically significant difference (p<0.05) was obtained for 45% and 76% of temperature bins in the aerosol and suspension measurements, respectively. This indicates that while the INA of unaged and aged samples may show similarities in certain specific temperature bins, both ANCOVA across temperatures and individual temperature bin statistical analyses provide strong quantitative evidence that the aging process leads to a change in the INA of the dust particles. For temperature bins where aging did not lead to significant differences, the underlying reason may be that aging effects vary depending on the aging treatments (Figure 6) or that specific mineral species are insensitive to aging (Figure S5). A detailed discussion on how different aging treatments influence the INA of different mineral dust is provided in section 3.3.

Table S5. Results of Mann-Whitney U-tests comparing the ice nucleation activity (INA) between unaged and aged dust samples in aerosol measurements.

Measurement	Temperature bins (°C)	P value	Significant difference
Aerosol	-42	-	Not enough data
Aerosol	-41	-	Not enough data
Aerosol	-40	>0.05	No
Aerosol	-39	>0.05	No
Aerosol	-38	<0.05	Yes
Aerosol	-37	<0.05	Yes
Aerosol	-36	<0.05	Yes
Aerosol	-35	>0.05	No
Aerosol	-34	>0.05	No
Aerosol	-33	>0.05	No
Aerosol	-32	<0.05	Yes
Aerosol	-31	>0.05	No
Aerosol	-30	<0.05	Yes
Aerosol	-29	<0.05	Yes
Aerosol	-28	>0.05	No
Aerosol	-27	>0.05	No
Aerosol	-26	>0.05	No
Aerosol	-25	<0.05	Yes

Aerosol	-24	<0.05	Yes
Aerosol	-23	-	Not enough data
Aerosol	-22	<0.05	Yes
Aerosol	-21	>0.05	No
Aerosol	-20	>0.05	No

Table S6. Results of non-parametric Mann-Whitney U-tests comparing the ice nucleation activity (INA) between unaged and aged dust samples in suspension measurements.

Measurement	Temperature bins (°C)	P value	Significant difference
Suspension	-38	-	Not enough data
Suspension	-37	-	Not enough data
Suspension	-36	-	Not enough data
Suspension	-35	-	Not enough data
Suspension	-34	-	Not enough data
Suspension	-33	-	Not enough data
Suspension	-32	-	Not enough data
Suspension	-31	-	Not enough data
Suspension	-30	-	Not enough data
Suspension	-29	-	Not enough data
Suspension	-28	-	Not enough data
Suspension	-27	<0.05	Yes
Suspension	-26	>0.05	No
Suspension	-25	>0.05	No
Suspension	-24	<0.05	Yes
Suspension	-23	<0.05	Yes
Suspension	-22	<0.05	Yes
Suspension	-21	<0.05	Yes
Suspension	-20	>0.05	No
Suspension	-19	<0.05	Yes
Suspension	-18	<0.05	Yes
Suspension	-17	<0.05	Yes

Suspension	-16	<0.05	Yes
Suspension	-15	<0.05	Yes
Suspension	-14	<0.05	Yes
Suspension	-13	<0.05	Yes
Suspension	-12	<0.05	Yes
Suspension	-11	<0.05	Yes
Suspension	-10	<0.05	Yes
Suspension	-9	<0.05	Yes
Suspension	-8	<0.05	Yes
Suspension	-7	<0.05	Yes
Suspension	-6	<0.05	Yes
Suspension	-5	>0.05	No
Suspension	-4	>0.05	No
Suspension	-3	>0.05	No

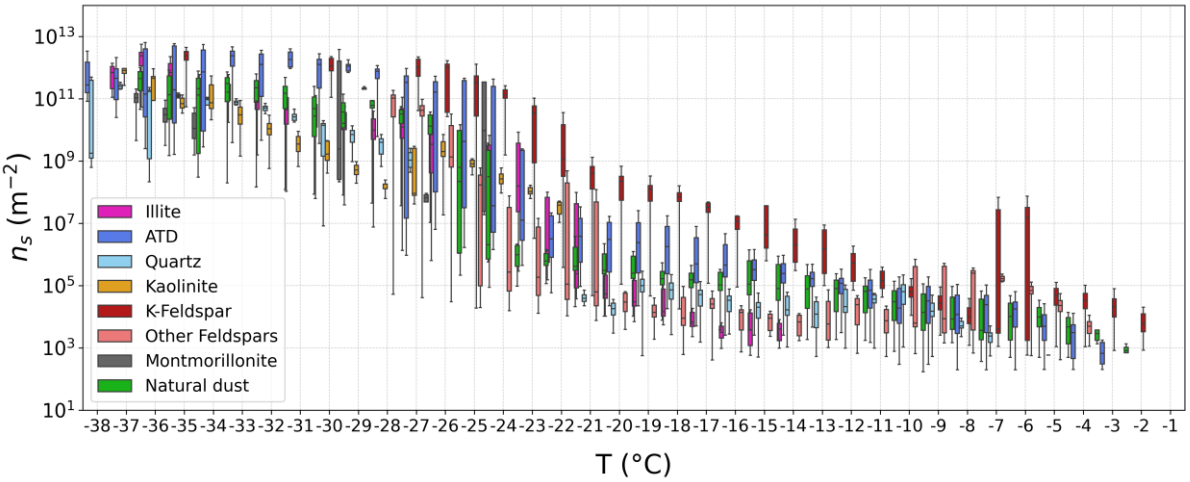


Figure S1. Boxplots of n_s for dust particles with different mineral compositions. n_s data were binned into 1 °C intervals at -38 < T <-2 °C. The box is not shown if the containing data points at each temperature bin are less than five.

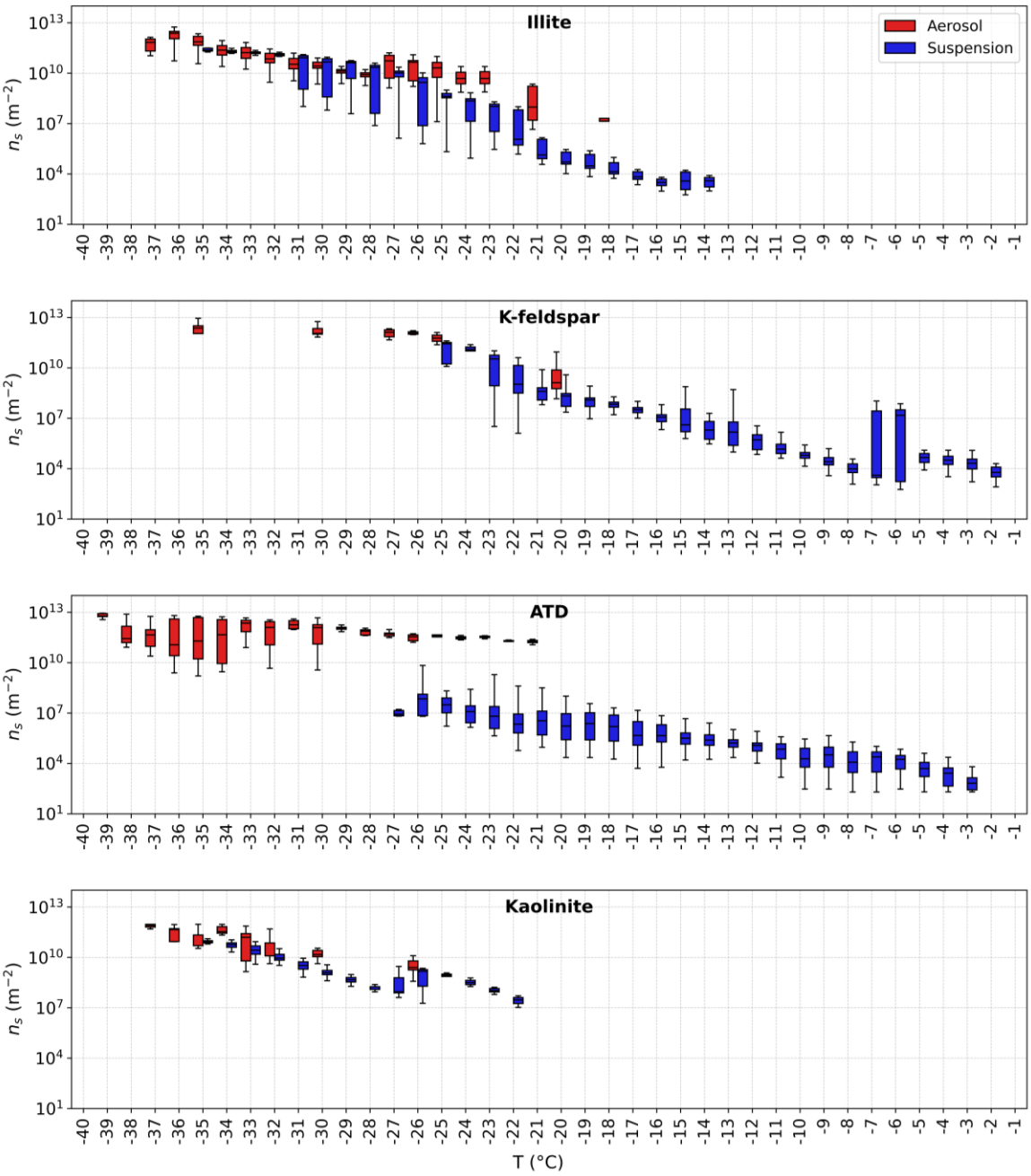


Figure S2. Boxplots of n_s dust particles with different mineral compositions measured from dry-dispersed particles (aerosol, red) and wet-suspended particles (suspension, blue). The n_s were binned into 1 ℃ intervals at -40 < T <-2 ℃. n_s of quartz, non-potassium feldspars and montmorillonite are not shown due to the lack of or inadequte data from aerosol measurements for each temperature bin.

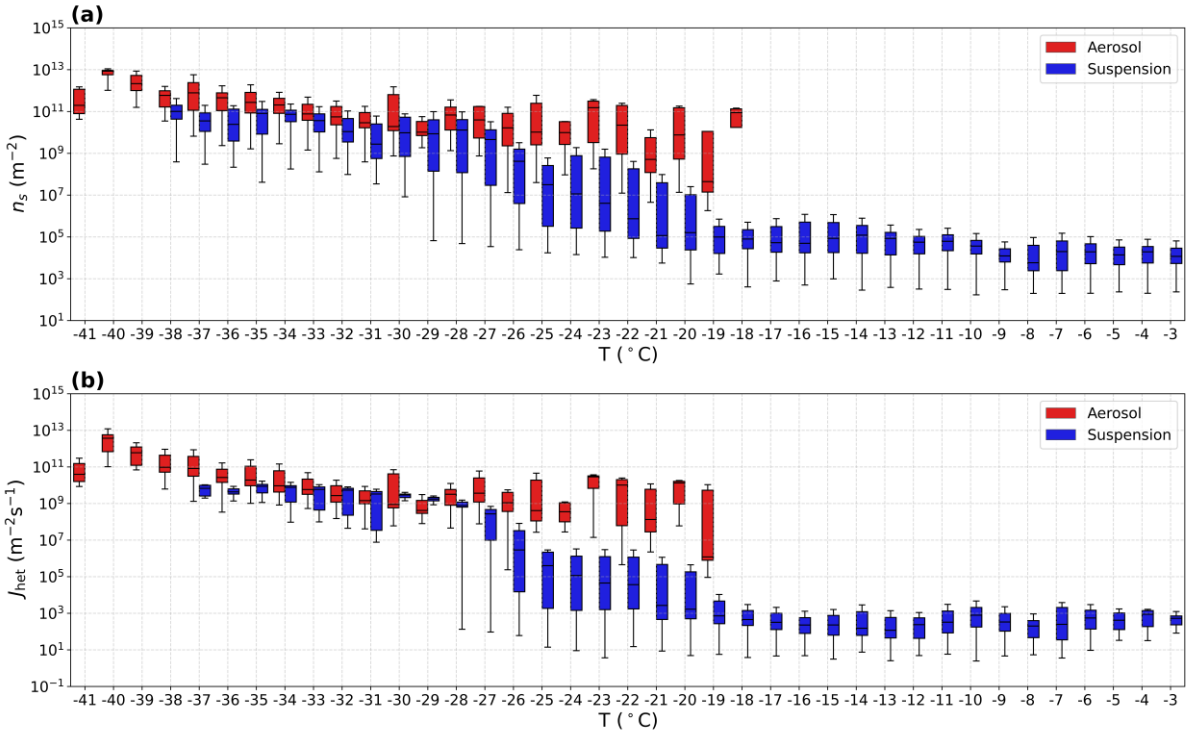


Figure S3. Boxplots of (a) n_s and (b) J_{het} of dust particles measured from dry-dispersed particles (aerosol, red) and wet-suspended particles (suspension, blue). The n_s and J_{het} data were binned into 1 °C intervals at -41 < T <-3 °C. There are fewer J_{het} data compared to n_s, as some studies did not provide sufficient information to derive J_{het}.

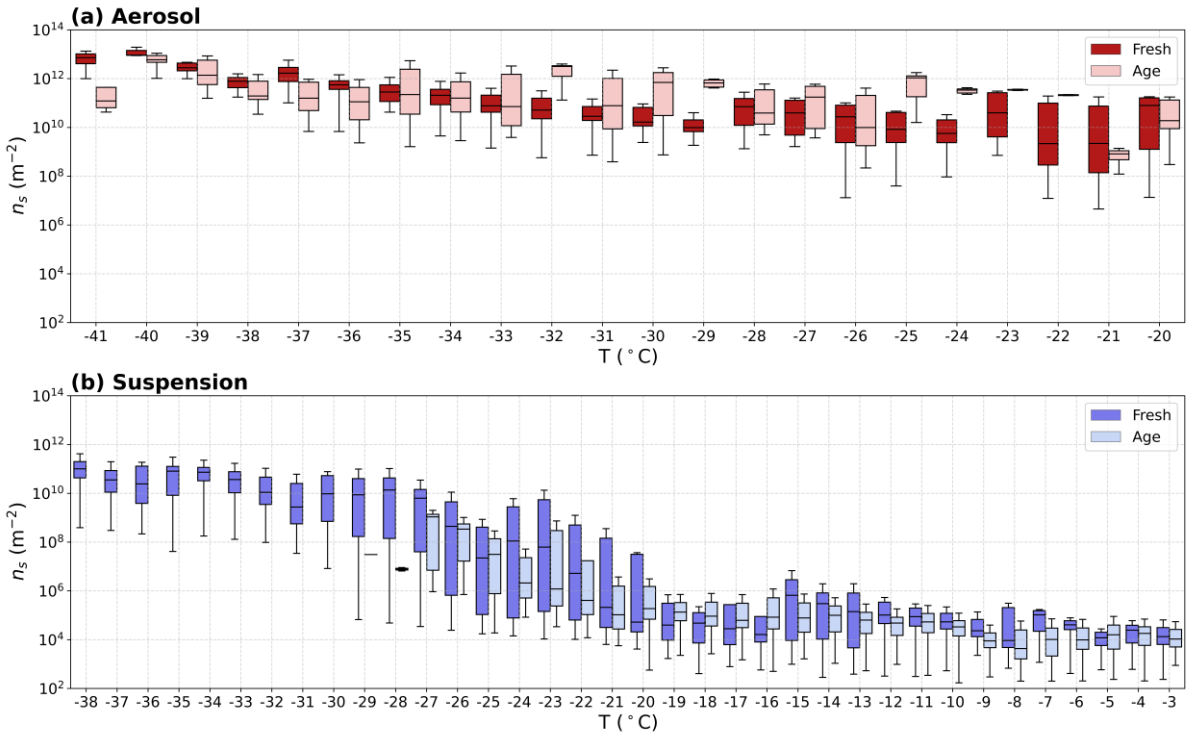


Figure S4. Boxplots of n_s for unaged (solid color, Fresh) and aged (faded color, Age) dust particles obtained from (a) aerosol and (b) suspension measurements. n_s data were binned into 1 °C intervals at -41 < T <-3 °C for aerosol measurements and at -38 < T <-3 °C for suspension measurements.

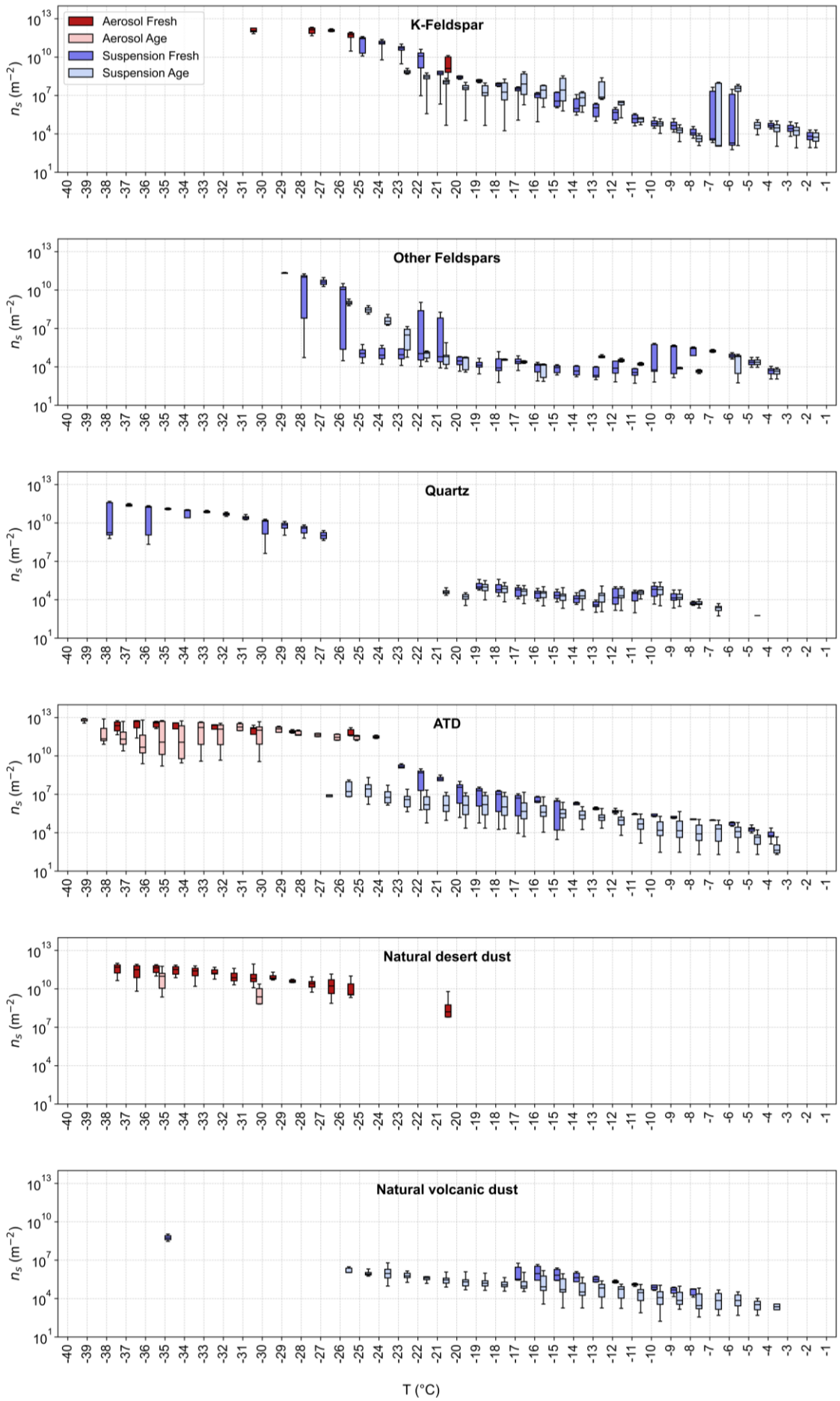

Aerosol Fresh
Aerosol Age
Suspension Fresh
Suspension Age
K-Feldspar
Other Feldspars
Quartz
ATD
Natural desert dust
Natural volcanic dust
n_s (m^{-2})
T (°C)

Figure S5. Boxplots of n_s for unaged (solid color, Fresh) and aged dust (faded color, Age) particles with different compositions, including K-feldspar, non-potassium-rich feldspar (other feldspars), quartz, ATD and natural dust (both desert dust and volcanic dust). The n_s data were binned into 1 ℃ intervals at -40 < T <-1 ℃.

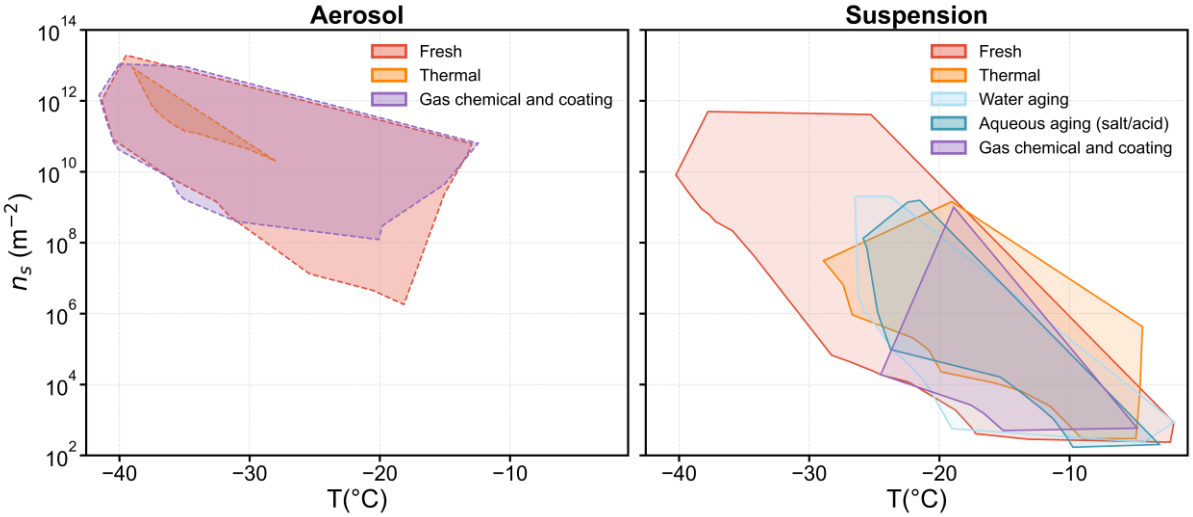


Figure S6. n_s of dust particles unaged (red shaded polygon, Fresh) and after various aging treatments, including water and aqueous aging, thermal treatments, chemical reactions with gas and coating by inorganic or organic compounds (denoted as gas chemical and coating). This figure compiles the complete n_s data from different studies, including those reporting only the INA of unaged dust particles. For comparison, Figure 6 presents n_s data from selected studies in which both unaged and aged dust particles of the same type were measured.

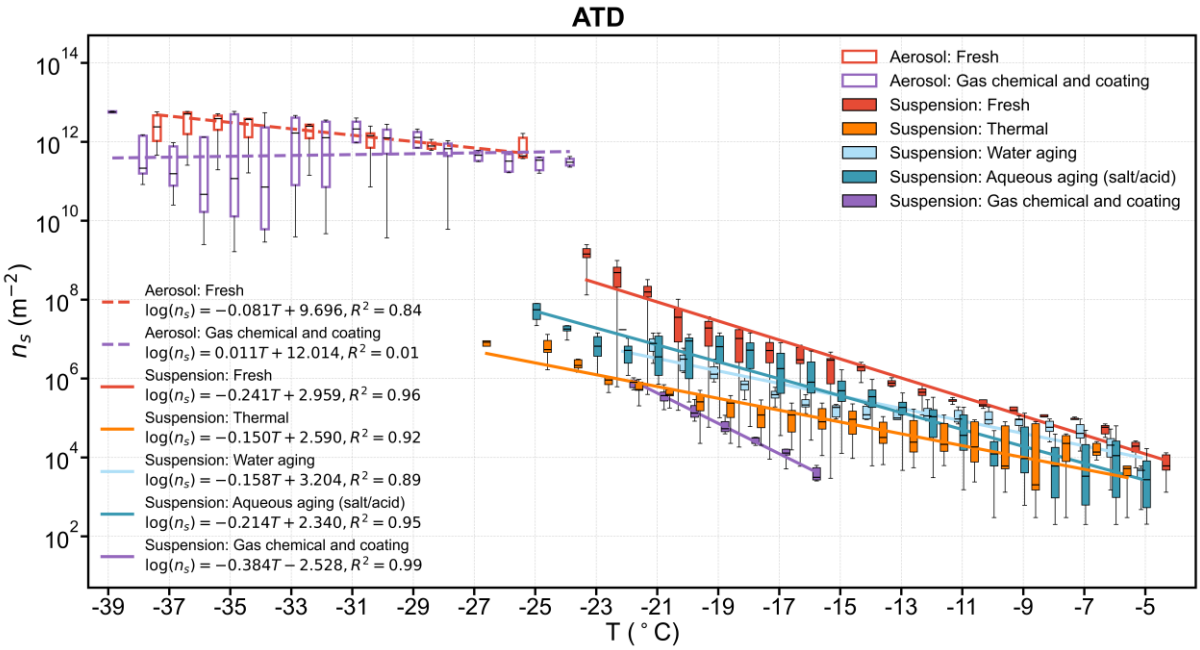


Figure S7. n_s of unaged ATD particles (red, Fresh) and after undergoing various aging processes, including water aging (light blue), aqueous aging (dark blue), thermal treatment (orange), gas chemical reactions and coating (purple). Dataset of dry-dispersed aerosol (hollow box) and wet-suspended particles (solid box) are displayed separately. The parameterizations used to predict n_s of ATD particles

aged through different processes are of the form: $log(n_s) = A \times T + B$. The values of fitted parameter A and B are indicated in this figure.

References

Atkinson, J. D., Murray, B. J., Woodhouse, M. T., Whale, T. F., Baustian, K. J., Carslaw, K. S., Dobbie, S., O'sullivan, D., and Malkin, T. L.: The importance of feldspar for ice nucleation by mineral dust in mixed-phase clouds, Nature, 498, 355, https://doi.org/10.1038/nature12278, 2013.

Augustin-Bauditz, S., Wex, H., Kanter, S., Ebert, M., Niedermeier, D., Stolz, F., Prager, A., and Stratmann, F.: The immersion mode ice nucleation behavior of mineral dusts: A comparison of different pure and surface modified dusts, Geophysical Research Letters, 41, 7375–7382, https://doi.org/10.1002/2014GL061317, 2014.

Boose, Y., Welti, A., Atkinson, J., Ramelli, F., Danielczok, A., Bingemer, H. G., Ploetze, M., Sierau, B., Kanji, Z. A., and Lohmann, U.: Heterogeneous ice nucleation on dust particles sourced from nine deserts worldwide-Part 1: Immersion freezing, Atmospheric Chemistry and Physics, 16, https://doi.org/10.5194/acp-16-15075-2016, 2016.

Broadley, S. L., Murray, B. J., Herbert, R. J., Atkinson, J. D., Dobbie, S., Malkin, T. L., Condliffe, E., and Neve, L.: Immersion mode heterogeneous ice nucleation by an illite rich powder representative of atmospheric mineral dust, Atmospheric Chemistry and Physics, 12, 287–307, https://doi.org/10.5194/acp-12-287-2012, 2012.

Chen, J. P., Hazra, A., and Levin, Z.: Parameterizing ice nucleation rates using contact angle and activation energy derived from laboratory data, Atmospheric Chemistry and Physics, 8, 7431–7449, https://doi.org/10.5194/acp-8-7431-2008, 2008.

Chen, L., Peng, C., Chen, J., Chen, J., Gu, W., Jia, X., Wu, Z., Wang, Q., and Tang, M.: Effects of heterogeneous reaction with NO2 on ice nucleation activities of feldspar and Arizona Test Dust, Journal of Environmental Sciences, 127, 210–221, https://doi.org/10.1016/j.jes.2022.04.034, 2023.

DeMott, P. J., Möhler, O., Cziczo, D. J., Hiranuma, N., Petters, M. D., Petters, S. S., Belosi, F., Bingemer, H. G., Brooks, S. D., and Budke, C.: The Fifth InternationalWorkshop on Ice Nucleation phase 2 (FIN-02): laboratory intercomparison of ice nucleation measurements, Atmospheric Measurement Techniques, 11, 6231–6257, https://doi.org/10.5194/amt-2018-191, 2018.

DeMott, P. J., Prenni, A. J., McMeeking, G. R., Sullivan, R. C., Petters, M. D., Tobo, Y., Niemand, M., Möhler, O., Snider, J. R., Wang, Z., and Kreidenweis, S. M.: Integrating laboratory and field data to quantify the immersion freezing ice nucleation activity of mineral dust particles, Atmospheric Chemistry and Physics, 15, 393–409, https://doi.org/10.5194/acp-15-393-2015, 2015.

Emersic, C., Connolly, P. J., Boult, S., Campana, M., and Li, Z.: Investigating the discrepancy between wet-suspension- and dry-dispersion-derived ice nucleation efficiency of mineral particles, Atmospheric Chemistry and Physics, 15, 11311–11326, https://doi.org/10.5194/acp-15-11311-2015, 2015.

Fahy, W. D., Maters, E. C., Giese Miranda, R., Adams, M. P., Jahn, L. G., Sullivan, R. C., and Murray, B. J.: Volcanic ash ice nucleation activity is variably reduced by aging in water and sulfuric acid: the effects of leaching, dissolution, and precipitation, Environmental Science: Atmospheres, 2, 85–99, https://doi.org/10.1039/D1EA00071C, 2022.

Harrison, A. D., Lever, K., Sanchez-Marroquin, A., Holden, M. A., Whale, T. F., Tarn, M. D., McQuaid, J. B., and Murray, B. J.: The ice-nucleating ability of quartz immersed in water and its atmospheric importance compared to K-feldspar, Atmospheric Chemistry and Physics, 19, 11343–11361, https://doi.org/10.5194/acp-19-11343-2019, 2019.

Harrison, A. D., Whale, T. F., Carpenter, M. A., Holden, M. A., Neve, L., apos, Sullivan, D., Vergara Temprado, J., and Murray, B. J.: Not all feldspars are equal: a survey of ice nucleating properties across the feldspar group of minerals, Atmospheric Chemistry and Physics, 16, 10927–10940, https://doi.org/10.5194/acp-16-10927-2016, 2016.

Hiranuma, N., Augustin-Bauditz, S., Bingemer, H., Budke, C., Curtius, J., Danielczok, A., Diehl, K., Dreischmeier, K., Ebert, M., Frank, F., Hoffmann, N., Kandler, K., Kiselev, A., Koop, T., Leisner, T., Möhler, O., Nillius, B., Peckhaus, A., Rose, D., Weinbruch, S., Wex, H., Boose, Y., DeMott, P. J., Hader, J. D., Hill, T. C. J., Kanji, Z. A., Kulkarni, G., Levin, E. J. T., McCluskey, C. S., Murakami, M., Murray, B. J., Niedermeier, D., Petters, M. D., O'Sullivan, D., Saito, A., Schill, G. P., Tajiri, T., Tolbert, M. A., Welti, A., Whale, T. F., Wright, T. P., and Yamashita, K.: A comprehensive laboratory study on the immersion freezing behavior of illite NX particles: a comparison of 17 ice nucleation measurement techniques, Atmospheric Chemistry and Physics, 15, 2489–2518, https://doi.org/10.5194/acp-15-2489-2015, 2015.

Kanji, Z., Welti, A., Chou, C., Stetzer, O., and Lohmann, U.: Laboratory studies of immersion and deposition mode ice nucleation of ozone aged mineral dust particles, Atmospheric Chemistry and Physics, 13, 9097–9118, https://doi.org/10.5194/acp-13-9097-2013, 2013a.

Kanji, Z. A., Welti, A., Chou, C., Stetzer, O., and Lohmann, U.: Laboratory studies of immersion and deposition mode ice nucleation of ozone aged mineral dust particles, Atmospheric Chemistry and Physics, 13, 9097–9118, https://doi.org/10.5194/acp-13-9097-2013, 2013b.

Kanji, Z. A., Sullivan, R. C., Niemand, M., DeMott, P. J., Prenni, A. J., Chou, C., Saathoff, H., and Möhler, O.: Heterogeneous ice nucleation properties of natural desert dust particles coated with a surrogate of secondary organic aerosol, Atmospheric Chemistry and Physics, 19, 5091–5110, https://doi.org/10.5194/acp-19-5091-2019, 2019.

Kulkarni, G., Sanders, C., Zhang, K., Liu, X., and Zhao, C.: Ice nucleation of bare and sulfuric acid-coated mineral dust particles and implication for cloud properties, Journal of Geophysical Research: Atmospheres, 119, 9993–10011, https://doi.org/10.1002/2014JD021567, 2014.

Kulkarni, G., Zhang, K., Zhao, C., Nandasiri, M., Shutthanandan, V., Liu, X., Fast, J., and Berg, L.: Ice formation on nitric acid-coated dust particles: Laboratory and modeling studies, Journal of Geophysical Research: Atmospheres, 120, 7682–7698, https://doi.org/10.1002/2014JD022637, 2015.

Marcolli, C., Gedamke, S., Peter, T., and Zobrist, B.: Efficiency of immersion mode ice nucleation on surrogates of mineral dust, Atmospheric Chemistry and Physics, 7, 5081–5091, https://doi.org/10.5194/acp-7-5081-2007, 2007.

Murray, B. J., Broadley, S. L., Wilson, T. W., Atkinson, J. D., and Wills, R. H.: Heterogeneous freezing of water droplets containing kaolinite particles, Atmospheric Chemistry and Physics, 11, 4191–4207, https://doi.org/10.5194/acp-11-4191-2011, 2011.

Niedermeier, D., Shaw, R. A., Hartmann, S., Wex, H., Clauss, T., Voigtländer, J., and Stratmann, F.: Heterogeneous ice nucleation: exploring the transition from stochastic to singular freezing behavior, Atmospheric Chemistry and Physics, 11, 8767–8775, https://doi.org/10.5194/acp-11-8767-2011, 2011a.

Niedermeier, D., Hartmann, S., Clauss, T., Wex, H., Kiselev, A., Sullivan, R., DeMott, P., Petters, M., Reitz, P., and Schneider, J.: Experimental study of the role of physicochemical surface processing on the IN ability of mineral dust particles, Atmospheric Chemistry and Physics, 11, 11131–11144, https://doi.org/10.5194/acp-11-11131-2011, 2011b.

Niemand, M., Möhler, O., Vogel, B., Vogel, H., Hoose, C., Connolly, P., Klein, H., Bingemer, H., DeMott, P., and Skrotzki, J.: A particle-surface-area-based parameterization of immersion freezing on desert dust particles, Journal of the Atmospheric Sciences, 69, 3077–3092, https://doi.org/10.1175/jas-d-11-0249.1, 2012.

Peckhaus, A., Kiselev, A., Hiron, T., Ebert, M., and Leisner, T.: A comparative study of K-rich and Na/Ca-rich feldspar ice-nucleating particles in a nanoliter droplet freezing assay, Atmospheric Chemistry and Physics, 16, 11477–11496, https://doi.org/10.5194/acp-16-11477-2016, 2016.

Perkins, R. J., Gillette, S. M., Hill, T. C., and DeMott, P. J.: The labile nature of ice nucleation by Arizona Test Dust, ACS Earth and Space Chemistry, 4, 133–141, https://doi.org/10.1021/acsearthspacechem.9b00304, 2019.

Salam, A., Lohmann, U., and Lesins, G.: Ice nucleation of ammonia gas exposed montmorillonite mineral dust particles, Atmospheric Chemistry and Physics, 7, 3923–3931, https://doi.org/10.5194/acp-7-3923-2007, 2007.

Savre, J. and Ekman, A. M. L.: A theory-based parameterization for heterogeneous ice nucleation and implications for the simulation of ice processes in atmospheric models, Journal of Geophysical Research: Atmospheres, 120, 4937–4961, https://doi.org/10.1002/2014JD023000, 2015.

Sihvonen, S. K., Schill, G. P., Lyktey, N. A., Veghte, D. P., Tolbert, M. A., and Freedman, M. A.: Chemical and physical transformations of aluminosilicate clay minerals due to acid treatment and consequences for heterogeneous ice nucleation, The Journal of Chemical Physics A, 118, 8787–8796, https://doi.org/10.1021/jp504846g, 2014.

Sullivan, R. C., Miñambres, L., DeMott, P. J., Prenni, A. J., Carrico, C. M., Levin, E. J. T., and Kreidenweis, S. M.: Chemical processing does not always impair heterogeneous ice nucleation of mineral dust particles, Geophysical Research Letters, 37, https://doi.org/10.1029/2010GL045540, 2010a.

Sullivan, R. C., Petters, M. D., DeMott, P. J., Kreidenweis, S. M., Wex, H., Niedermeier, D., Hartmann, S., Clauss, T., Stratmann, F., Reitz, P., Schneider, J., and Sierau, B.: Irreversible loss of ice nucleation active sites in mineral dust particles caused by sulphuric acid condensation, Atmospheric Chemistry and Physics, 10, 11471–11487, https://doi.org/10.5194/acp-10-11471-2010, 2010b.

Tobo, Y., DeMott, P. J., Raddatz, M., Niedermeier, D., Hartmann, S., Kreidenweis, S. M., Stratmann, F., and Wex, H.: Impacts of chemical reactivity on ice nucleation of kaolinite particles: A case study of levoglucosan and sulfuric acid, Geophysical Research Letters, 39, https://doi.org/10.1029/2012GL053007, 2012.

Ullrich, R., Hoose, C., Möhler, O., Niemand, M., Wagner, R., Höhler, K., Hiranuma, N., Saathoff, H., and Leisner, T.: A New Ice Nucleation Active Site Parameterization for Desert Dust and Soot, Journal of the Atmospheric Sciences, 74, 699–717, https://doi.org/10.1175/JAS-D-16-0074.1, 2017.

Wex, H., DeMott, P. J., Tobo, Y., Hartmann, S., Rösch, M., Clauss, T., Tomsche, L., Niedermeier, D., and Stratmann, F.: Kaolinite particles as ice nuclei: learning from the use of different kaolinite samples and different coatings, Atmospheric Chemistry and Physics, 14, 5529–5546, https://doi.org/10.5194/acp-14-5529-2014, 2014.

Zolles, T., Burkart, J., Häusler, T., Pummer, B., Hitzenberger, R., and Grothe, H.: Identification of ice nucleation active sites on feldspar dust particles, The Journal of Chemical Physics, 119, 2692–2700, https://doi.org/10.1021/jp509839x, 2015.